



Article

Cryo-Treatment Enhances the Embryogenicity of Mature Somatic Embryos via the lncRNA–miRNA–mRNA Network in White Spruce

Ying Gao ^{1,†}, Ying Cui ^{1,†}, Ruirui Zhao ¹, Xiaoyi Chen ¹, Jinfeng Zhang ¹, Jian Zhao ^{1,*} and Lisheng Kong ^{1,2,*}

- ¹ National Engineering Laboratory for Tree Breeding, Key Laboratory of Genetics and Breeding in Forest Trees and Ornamental Plants, Ministry of Education, The Tree and Ornamental Plant Breeding and Biotechnology Laboratory of National Forestry and Grassland Administration, College of Biological Sciences and Biotechnology, Beijing Forestry University, Beijing 100083, China; gying@zju.edu.cn (Y.G.); cwfpyl@163.com (Y.C.); zhaorui1012@gmail.com (R.Z.); cxy919@bjfu.edu.cn (X.C.); zjf@bjfu.edu.cn (J.Z.)
- ² Centre for Forest Biology, Department of Biology, University of Victoria, Victoria, BC V8W 3N5, Canada
- * Correspondence: zhaojian0703@bjfu.edu.cn (J.Z.); lkong@uvic.ca (L.K.)
- † These authors contributed equally to this work.

Abstract: In conifers, somatic embryogenesis is uniquely initiated from immature embryos in a narrow time window, which is considerably hindered by the difficulty to induce embryogenic tissue (ET) from other tissues, including mature somatic embryos. In this study, the embryogenic ability of newly induced ET and DNA methylation levels was detected, and whole-transcriptome sequencing analyses were carried out. The results showed that ultra-low temperature treatment significantly enhanced ET induction from mature somatic embryos, with the induction rate from 0.4% to 15.5%, but the underlying mechanisms remain unclear. The newly induced ET showed higher capability in generating mature embryos than the original ET. DNA methylation levels fluctuated during the ET induction process. Here, WGCNA analysis revealed that *OPT4*, *TIP1-1*, *Chi I*, *GASA5*, *GST*, *LAX3*, *WRKY7*, *MYBS3*, *LRR-RLK*, *PBL7*, and *WIN1* genes are involved in stress response and auxin signal transduction. Through co-expression analysis, lncRNAs MSTRG.505746.1, MSTRG.1070680.1, and MSTRG.33602.1 might bind to pre-novel_miR_339 to promote the expression of *WRKY7* genes for stress response; *LAX3* could be protected by lncRNAs MSTRG.1070680.1 and MSTRG.33602.1 via serving as sponges for novel_miR_495 to initiate auxin signal transduction; lncRNAs MSTRG.505746.1, MSTRG.1070680.1, and MSTRG.33602.1 might serve as sponges for novel_miR_527 to enhance the expression of *Chi I* for early somatic embryo development. This study provides new insight into the area of stress-enhanced early somatic embryogenesis in conifers, which is also attributable to practical applications.

Keywords: liquid nitrogen; cryo-treated mature somatic embryos; whole transcriptome; lncRNAs; miRNAs; conifer



Citation: Gao, Y.; Cui, Y.; Zhao, R.; Chen, X.; Zhang, J.; Zhao, J.; Kong, L. Cryo-Treatment Enhances the Embryogenicity of Mature Somatic Embryos via the lncRNA–miRNA–mRNA Network in White Spruce. *Int. J. Mol. Sci.* **2022**, *23*, 1111. <https://doi.org/10.3390/ijms23031111>

Academic Editor:
Pedro Martínez-Gómez

Received: 15 December 2021
Accepted: 14 January 2022
Published: 20 January 2022

Publisher's Note: MDPI stays neutral with regard to jurisdictional claims in published maps and institutional affiliations.



Copyright: © 2022 by the authors. Licensee MDPI, Basel, Switzerland. This article is an open access article distributed under the terms and conditions of the Creative Commons Attribution (CC BY) license (<https://creativecommons.org/licenses/by/4.0/>).

1. Introduction

Conifers are important forest species, which are hard to be propagated via organogenesis due to the difficulty in root induction, while somatic embryogenesis provides an efficient propagation means [1,2]. In order to initiate somatic embryogenesis, immature zygotic embryos were commonly used as explants to induce embryogenic tissue (ET) in conifers. The embryogenicity of embryos declines with the increase in the degree of embryo maturation [3,4]. Though ET could be induced from mature zygotic embryos in very few coniferous species [5,6], the induction rate is generally low. Thus, the window of ET induction is important and limited by suitable embryo developmental stages, which are influenced by the weather in different years.

Cryopreservation is an important technology for the mass production of elite coniferous species [3,4]. Embryogenic materials need to be stored in liquid nitrogen during

the period of time for genotype selection. Immature somatic embryos possess high embryogenicity but no tolerance to ultra-low temperature without treatment with cryoprotectants [7]. In our previous study, mature somatic embryos of white spruce could be stored in liquid nitrogen without additional treatment, although their embryogenicity is low [8].

Though fresh mature somatic embryos could be available in large quantity and cryopreserved, ET consisting of immature somatic embryos is the preferred material for germplasm conservation and the initial tissue for mass propagation via somatic embryogenesis [9,10]. This is mainly due to the low embryogenicity of mature somatic embryos [4,8]. In the current study, we sought to determine where ET induction from mature somatic embryos could be increased largely in white spruce by cryo-treating the explants with liquid nitrogen. This discovery could enable mature somatic embryos to serve as germplasm materials in white spruce or conifers. It is well known that stress treatments could enhance the embryogenicity of the explants [11,12]. Little information is available about the mechanism of positive reactions of somatic embryogenesis induction enhanced by stress treatments, specifically ultra-low temperature, applied to the explants.

The developed transcriptome technologies revealed that only a small percent of transcribed genomes is attributed to protein-coding mRNAs in the eukaryotic body [13]. The other part of RNAs is called noncoding RNAs (ncRNAs), including ribosomal RNAs (rRNAs), transfer RNAs (tRNAs), small interfering RNAs (siRNAs), small nucleolar RNAs (snoRNAs), microRNAs (miRNAs), long noncoding RNAs (lncRNAs), and circular RNAs (circRNAs) [13–15]. Among various groups of ncRNAs, miRNAs [16], lncRNAs [17], and circRNAs [18] are known as regulatory ncRNAs. In plants, these ncRNAs play important roles in stress response [19,20] and the process of somatic embryogenesis [21] via regulating mRNAs directly or indirectly [22,23]. For example, miR172a could cleave AP2 domain-containing genes and promote thiamine biosynthesis gene expression, to improve salinity tolerance in soybean [24]. In *Medicago truncatula*, LNC_016398-MiCIR1 regulates the expression of CBF/DREB1 genes to respond to cold treatment [25]. *Vv-circATS1* is also related to cold resistance in grapes [26]. In *Valencia* sweet orange, miR156, 168, and 171 played important roles in somatic embryo induction [27]. Overexpression of miR167 hindered SE formation through the low expression of ARF6 and ARF8 in *Arabidopsis* [28]. During early somatic embryogenesis in *D. longan*, the lncRNA–miRNA–mRNA regulatory network with 15 miRNAs and 7 lncRNAs was constructed [21]. In maize, zma-miR528 could target several genes during somatic embryogenesis [29].

In conifers, miRNAs related to somatic embryogenesis have been studied on larch [30], Norway spruce [31], and *Picea balfouriana* [32]. Stress-related miRNAs were also reported in *Sabina chinensis* [33] and *Pinus pinaster* [34]. Unfortunately, the study of lncRNAs on the stress response and somatic embryogenesis has not been reported in conifers at present. In this study, RNA transcripts were obtained using high-throughput-sequencing technologies. Then, the regulatory network including mRNAs, miRNAs, and lncRNAs was analyzed with bioinformatics means, in order to explore the reason for inducing ET from cryo-treated mature somatic embryos and provide information for improving the efficacy of ET initiation, which is useful for elite conifer propagation via somatic embryogenesis.

2. Results

2.1. Morphological Changes during ET Induction

After recovering from liquid nitrogen, there were no obvious morphological differences between the cryo-treated mature somatic embryos (CRSEs) (Figure 1a) and the normal mature somatic embryo cultured at room temperature at 23 ± 1 °C (RTSE) (Figure 1b). During the early induction stage, the nucleus became visibly larger, and the ribosome depolymerized on day 1, as shown in Figure 2c,d. However, Figure 2c reveals that the partial nucleus did not change and was stained in dark red in CRSE. Five days later, the structure of CRSE became loose, and the bottom was obviously necrotic (Figure 2e), while RTSE began to swell, especially the cotyledons (Figure 2f). Subsequently, cells with large vacuoles appeared from the induction culture of CRSE on day 10 (Figure 2e), but the

cotyledons of RTSE were hard and malformed, and the callus without core was also small and dense, which is a marker for callus that is non-embryogenic (Figure 2f) [35]. Lastly, new embryogenic tissue (NET) was induced from CRSE on day 20 (Figure 1i), but there was no NET appearing on RTSE (Figure 1j). Additionally, the average induction rates of CRSE and RTSE were 15.5% and 0.4%, respectively (Figure 3a).

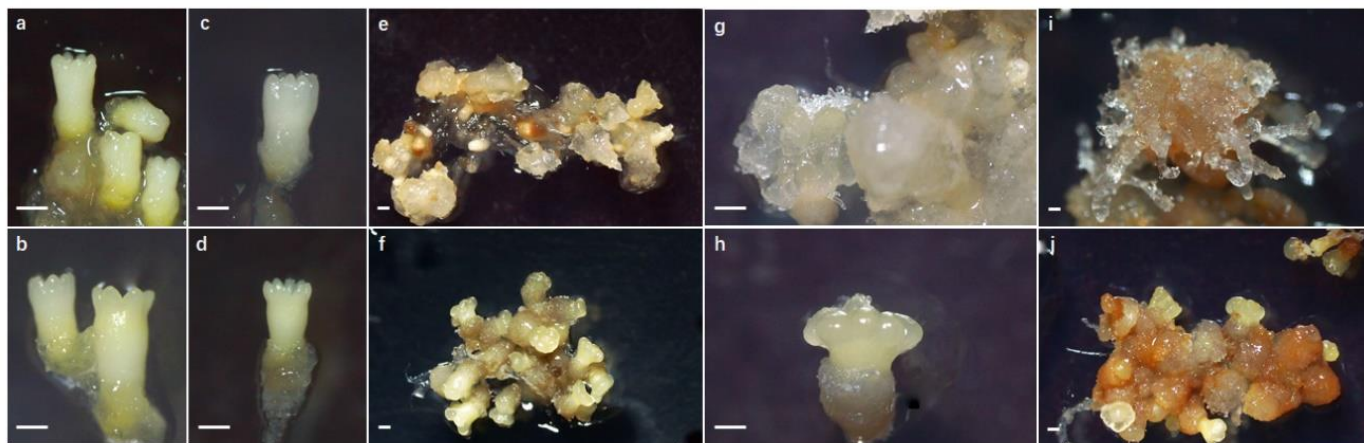


Figure 1. Induction process of cryo-treated mature somatic embryos (CRSEs) and normal mature somatic embryos cultured at room temperature (RTSEs): (a,c,e,g,i) show tissues sampled on day 0, 1, 10, 15, and 20 with explants of CRSE; (b,d,f,h,j) show tissues on day 0, 1, 10, 15, and 20 of RTSE. All bars = 500 μ m.

In order to detect the embryonic ability of NET, the ET and NET were cultured by pre-maturation and maturation medium at the same time after obtaining the NET from CRSE. As evident in Figure 3b, the embryonic ability of NET (1345 SE/g) was higher than that of the ET (995 SE/g). These results revealed that cryo-treatment could enhance the embryogenicity of mature somatic embryos, and the embryonic ability of NET induced from the cryo-treated mature somatic embryos was improved.

2.2. Differentially Expressed Genes (DEGs) and KEGG Analysis during the Induction Process

Non-coding RNAs exert special functions on the biological process via regulating targeted genes; therefore, DEGs were firstly analyzed in this study. Analysis showed that 9486 unigenes were screened by the criteria of $FDR < 0.05$ and $|\log_2(\text{fold change})| > 1$. Firstly, a sample cluster was applied for verifying repeatability among three biological replications and detecting affinity between different samples, including samples of day 0, 1, and 10 of the induction cultures of CRSE (CR0D, CR1D, CR10D) and RTSE (RT0D, RT1D, RT10D). As Figure 4a indicates, RT10D was firstly clustered together with RT1D, then clustered together with CR1D and CR10D, and lastly clustered together with CR0D (CRSE) and RT0D (RTSE), which corresponded with the change in explants during the induction process (Figures 1 and 2). All these also indicated that the transcriptomic results were reliable.

Hierarchical clustering (HCL) of DEGs analysis suggested that differentially expressed mRNAs were mainly divided into three types of expression profiles (Figure 4b). Obviously, most DEGs were highly expressed in the induction process of CRSE, while 2872 DEGs were highly expressed in the induction process of RTSE. Additionally, there were also 3083 DEGs similarly expressed in the induction process of CRSE and RTSE. Moreover, KEGG analysis results showed that DEGs were highly expressed in “ribosome” and “glycolysis/gluconeogenesis” during the induction process, especially at the stage of RT1D and CR1D, in which the ribosome depolymerized and dedifferentiation process started. Interestingly, DEGs enriched in “inositol phosphate metabolism” were specially expressed in CR10D (Figure 5). The results revealed that much more genes were activated during the ET induction process, especially genes related to inositol phosphate for signaling.

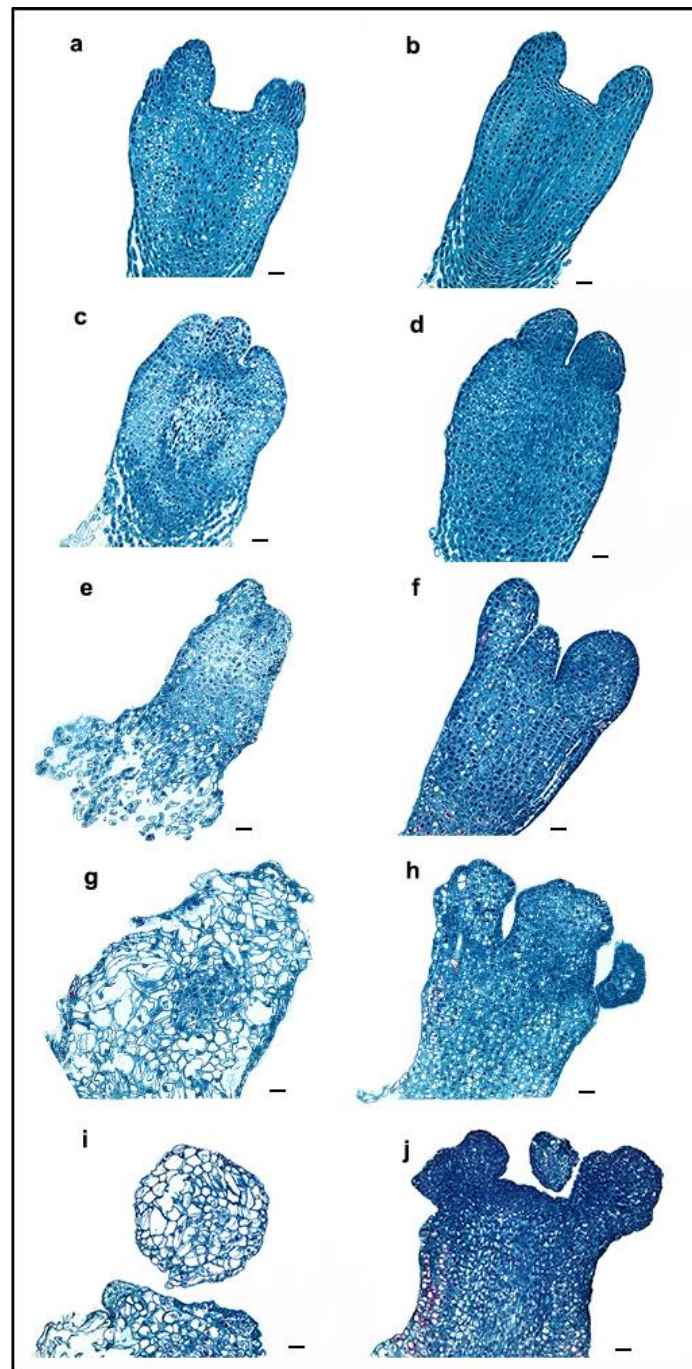


Figure 2. Microscopic observation of the change in cryo-treated mature somatic embryos (CRSEs) and normal mature somatic embryos cultured at room temperature (RTSEs) during callus induction: (a,c,e,g,i) show tissues sampled on day 0, 1, 5, 10, and 13 of CRSE; (b,d,f,h,j) show tissues sampled on day 0, 1, 5, 10, and 13 of RTSE. All bars = 50 μ m.

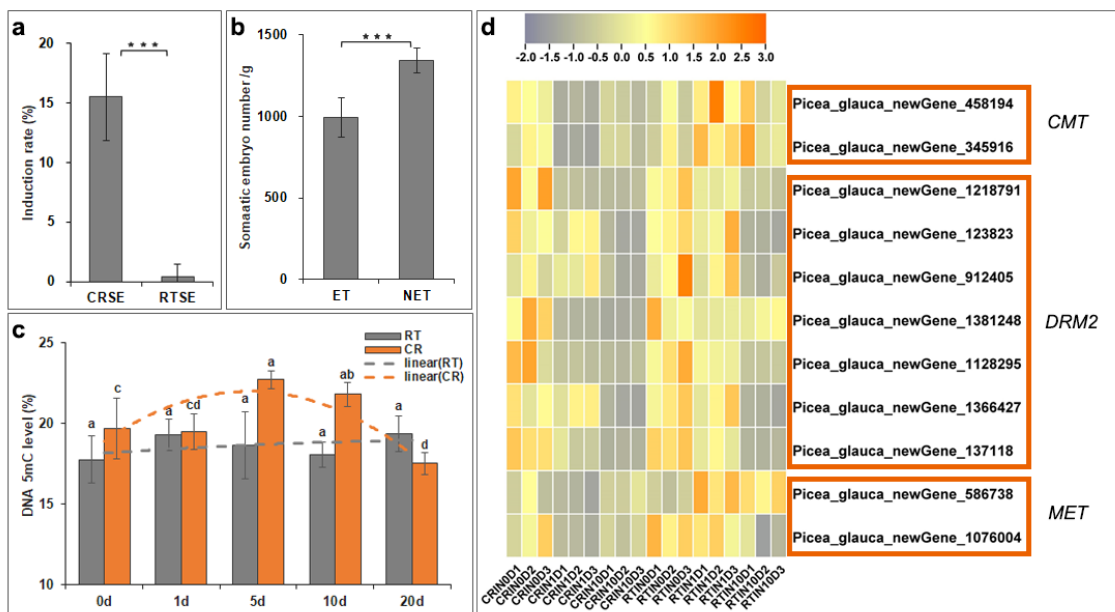


Figure 3. Induction rate, embryonic ability, DNA methylation level, and DNMTs expression heatmap: (a) average induction rate of CRSE and RTSE; (b) the total number of somatic embryos per gram of ET and NET; (c) global DNA methylation level of samples on day 0, 1, 5, 10, and 20 of CRSE (CR) and RTSE (RT); (d) heatmap of DNA methyltransferases genes *chromatinmethylase* (CMT), *domains rearranged methylase 2* (DRM2), and *methyltransferase* (MET). Asterisk and different letters represented significance ($p < 0.05$).

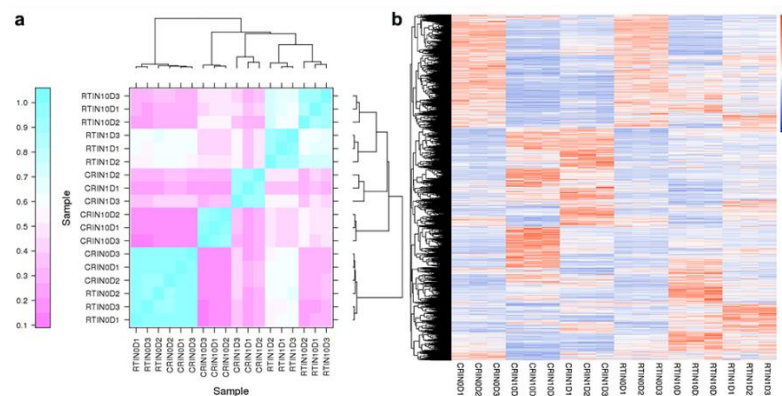


Figure 4. Analysis of differentially expressed mRNAs (DEGs): (a) sample cluster of 6 samples with three replicates, including CR0D, CR1D, CR10D, RT0D, RT1D, and RT10D; (b) cluster of DEGs in CR0D, CR1D, CR10D, RT0D, RT1D, and RT10D.

2.3. DNA Methylation Level Fluctuated during the Induction Process

Previous studies have shown that embryonic ability was closely related to DNA methylation [36]. In this study, the global DNA methylation at different induction stages was detected by HPLC to confirm whether DNA methylation was correlated with the induction process in white spruce (Figure 3c). DNA methylation level during the induction process with RTSE slightly altered from 17.5% to 19.4%. The DNA methylation level rose to 19.3% on the first day, then slightly reduced to 18.1% on day 10, and then sharply increased to 19.4% on day 20. Unlike RTSE, the trend of DNA methylation level during the induction from CRSE was saddle shaped. The highest level was 22.7% on the 5th day, then the DNA methylation level obviously decreased to 17.5% on the 20th day. The significantly increased DNA methylation level might be attributed to the stress response by cryo-treatment at the

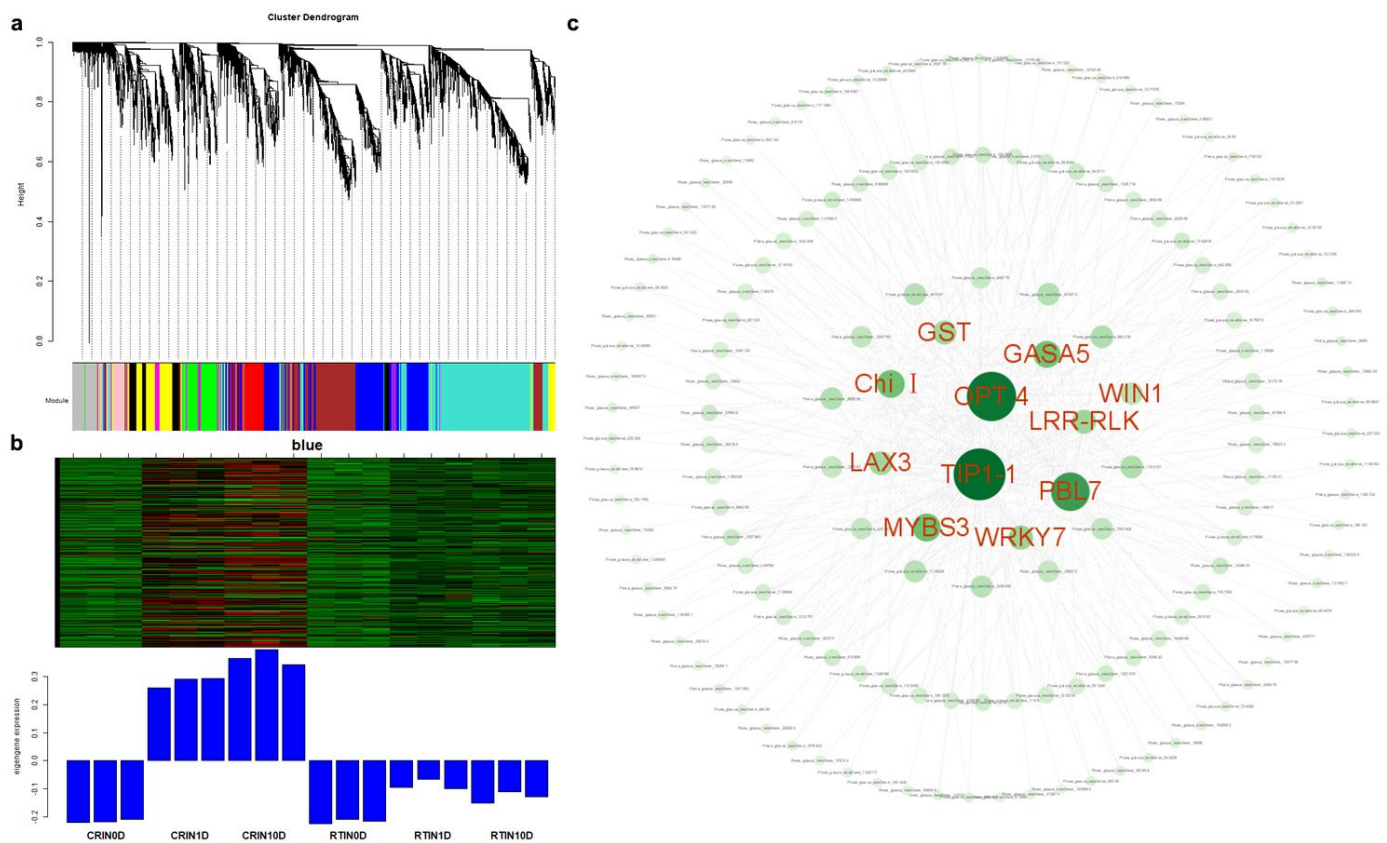


Figure 6. WGCNA analysis of DEGs: (a) cluster dendrogram of WGCNA analysis. Branches with different colors correspond to 10 different modules; (b) expression profile of DEGs in 6 samples of blue module; (c) network construction of DEGs in blue module, and 11 hub genes were selected in red font.

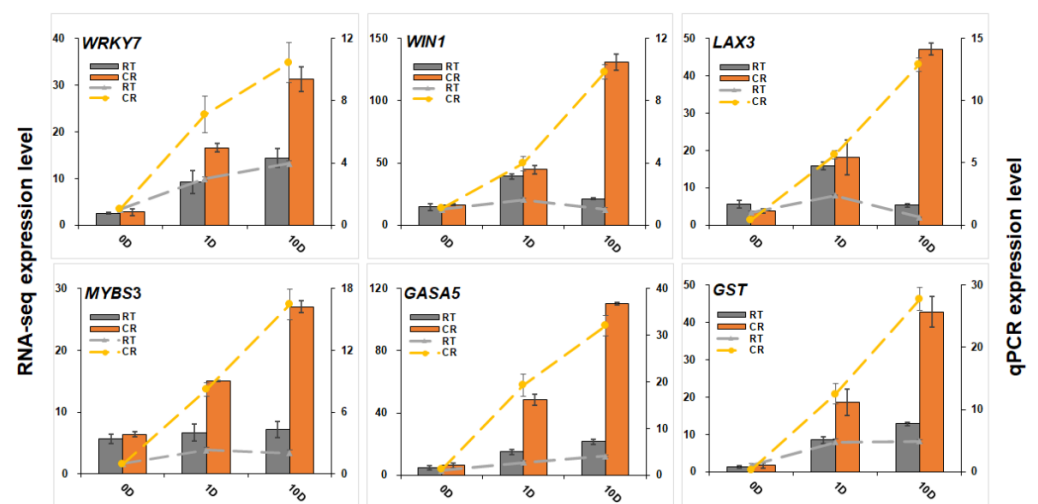


Figure 7. qPCR verification of mRNAs. qPCR results of WRKY transcription factor 7 (WRKY7), wound-induced protein WIN1 (WIN1), auxin transporter-like protein 3 (LAX3), Myb-related protein S3 (MYBS3), gibberellin-regulated protein 5 (GASA5), and glutathione S-transferase (GST). RT represents RTSE, and CR represents CRSE. The columns represent the RNA-seq expression level related to the left axis, while the lines represent the qPCR expression level correlated with the right axis.

2.5. Expression Profiles of lncRNAs and Construction of the lncRNA–mRNA Co-Expression Network

In total, 31,602 lncRNAs were identified, and 6271 lncRNAs were differentially expressed in 6 samples. Four comparison groups were set according to the differentiation stages of induction—namely, CR0D vs. CR1D, CR0D vs. CR10D, RT0D vs. RT1D, and RT0D vs. RT10D (Figure 8A). For CR0D vs. CR1D, 3921 lncRNAs were upregulated, and 3054 lncRNAs were downregulated (Figure 8A). For CR0D vs. CR10D, 5333 lncRNAs were upregulated, while 4199 lncRNAs were downregulated (Figure 4a). For RT0D vs. RT1D, 5252 lncRNAs were upregulated, and 3156 lncRNAs were downregulated (Figure 8a). For RT0D vs. RT10D, the number of up- and downregulated lncRNAs was 3599 and 4419, respectively (Figure 8A). All the differentially expressed lncRNAs were statistically significant ($p < 0.05$), with $|\text{fold change}| > 2.0$. VENN analysis revealed that 233 lncRNAs were upregulated and 863 lncRNAs were downregulated at all the stages during the induction process (Figure 8A). A cluster was generated and analyzed with hierarchical clustering for the often differentially regulated 132 lncRNAs (upregulated) and 786 lncRNAs (downregulated) in 6 samples (Figure 8B).

Based on the VENN analysis results, a co-expression network between lncRNA and mRNA belonging to blue modules was constructed. To this end, 235 pairs of lncRNA and mRNA relationships were determined with significant values of Pearson's correlation coefficients ($p < 0.05$) to generate a network map, containing 6 lncRNAs and 104 mRNAs. The final networks including 4 lncRNAs and 68 mRNAs and 187 relationships are presented in detail in Figure 8C. In the complex co-expression network, it is well known that one lncRNA could control multiple genes, and one gene could be correlated with multiple lncRNAs in different ways. From the network, we found that *OPT4*, *TIP1-1*, *Chi I*, *GST*, *WRKY7*, and *WIN1* genes were closely related to lncRNA MSTRG.33602.1, MSTRG.505746.1, and MSTRG.1070680.1. *LRR-RLK* was related to MSTRG.505746.1 and MSTRG.1070680.1, and *LAX 3* was related to MSTRG.1070680.1 and MSTRG.33602.1 (Figure 8D). MSTRG.33602.1, MSTRG.505746.1, and MSTRG.1070680.1 were detected by qPCR (Figure 9a). The expression profile of MSTRG.33602.1, MSTRG.505746.1, and MSTRG.1070680.1 also increased during the induction of CRSE, similar to *LRR-RLK*, *LAX3*, *OPT4*, *TIP1-1*, *Chi I*, *GST*, *WRKY7*, and *WIN1* genes.

2.6. Expression Profiles of miRNAs and Analysis of Targeted mRNA in the Blue Module

To further construct co-expressed miRNA–mRNA interaction, 995 differentially expressed miRNAs were analyzed. Among them, there were 465 conserved miRNAs and 531 novel miRNAs. Cluster results showed that the expression levels of 782 and 648 miRNAs were downregulated, respectively, during the cultivation of either CRSE or RTSE, while the expression levels of 213 and 347 miRNAs were upregulated, respectively, during the cultivation of CRSE or RTSE (Figure 10a). This network is more complex, compared with that of the lncRNA–mRNA relationship (Figure 10b). However, there still exists miRNA–hub gene regulation interaction during the process of induction. In our results, all the differentially expressed hub genes in the miRNA-targeted mRNA interaction were *WRKY7*, *LAX3*, and *Chi I* (Figure 10c). Among them, *WRKY7* was targeted by pab-miR391c, pab-miR3627d, and novel_miR_339, and *LAX3* was regulated by novel_miR_495, and *Chi I* was related to novel_miR_527. Then, novel_miR_339, novel_miR_495, and novel_miR_527 were verified by qPCR (Figure 9b). The expression of novel_miR_495 and novel_miR_527 decreased during the NET induction, but the expression of novel_miR_339 was not negatively correlated with targeted gene *WRKY7*.

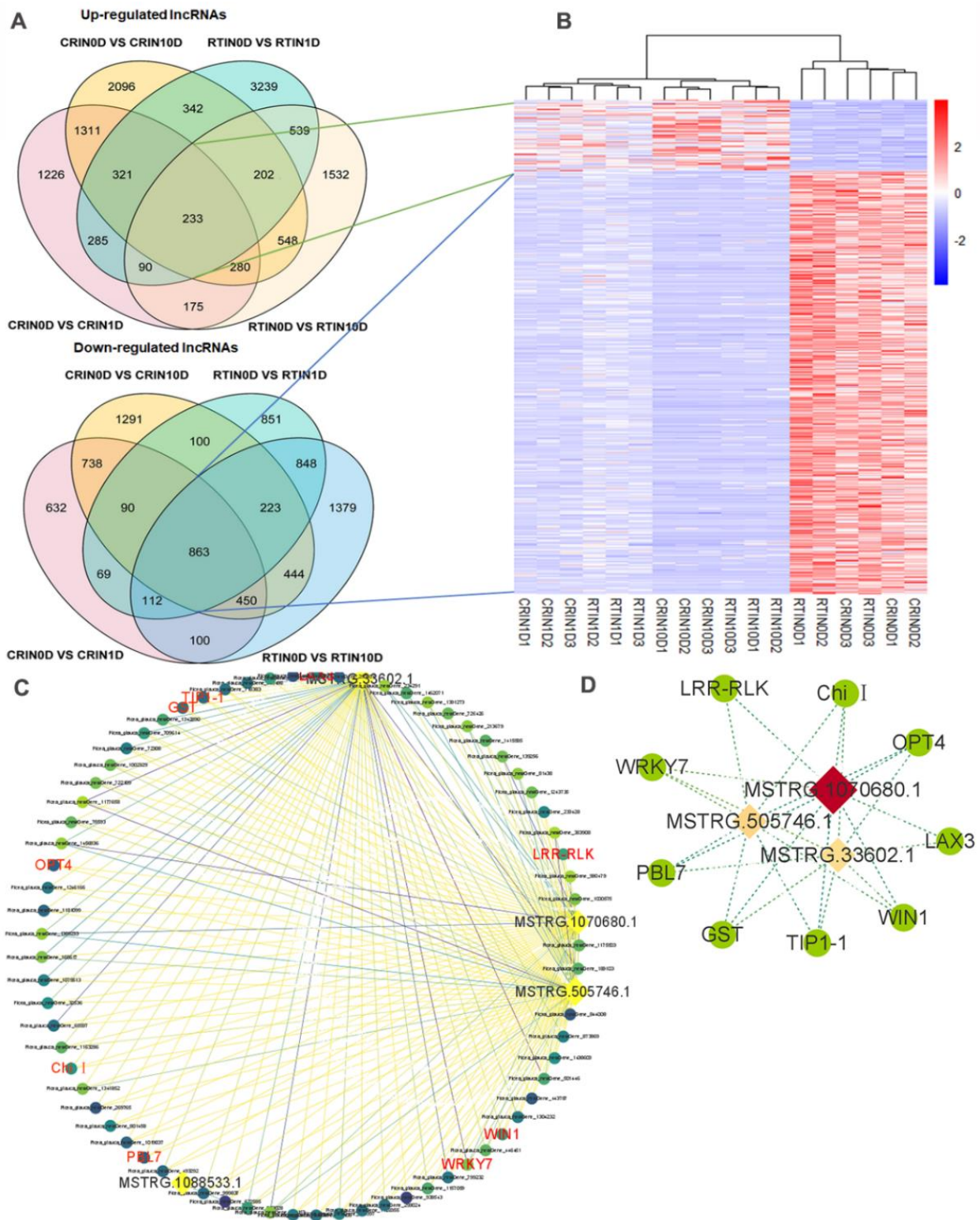


Figure 8. Co-expression analysis of lncRNAs and mRNAs in blue module of WGCNA results: (A) Venn analysis of up- and downregulated DElncRNAs of CR0D vs. CR1D, CR0D vs. CR10D, RT0D vs. RT1D, and RT0D vs. RT10D; (B) cluster analysis of the common lncRNAs in Venn analysis; (C) Co-expression network of lncRNAs and mRNAs in blue module; the color of circle and line represent coefficient and *p*-value, respectively; (D) Co-expression network of lncRNAs and hub genes; the color of diamond represents coefficient.

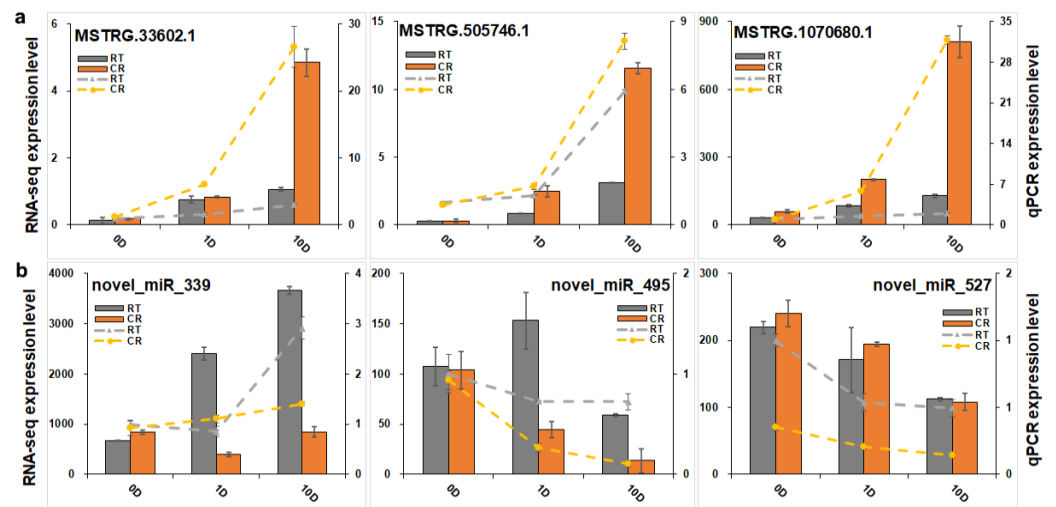


Figure 9. qPCR verification of lncRNAs and miRNAs: (a) qPCR verification of 3 lncRNAs, including MSTRG.33602.1, MSTRG.505746.1, and MSTRG.1070680.1; (b) qPCR verification of 3 miRNAs, including novel_miR_339, novel_miR_495, and novel_miR_527. RT represents RTSE, and CR represents CRSE. The columns represent the RNA-seq expression level related to the left axis, while the lines represent the qPCR expression level correlated with the right axis.

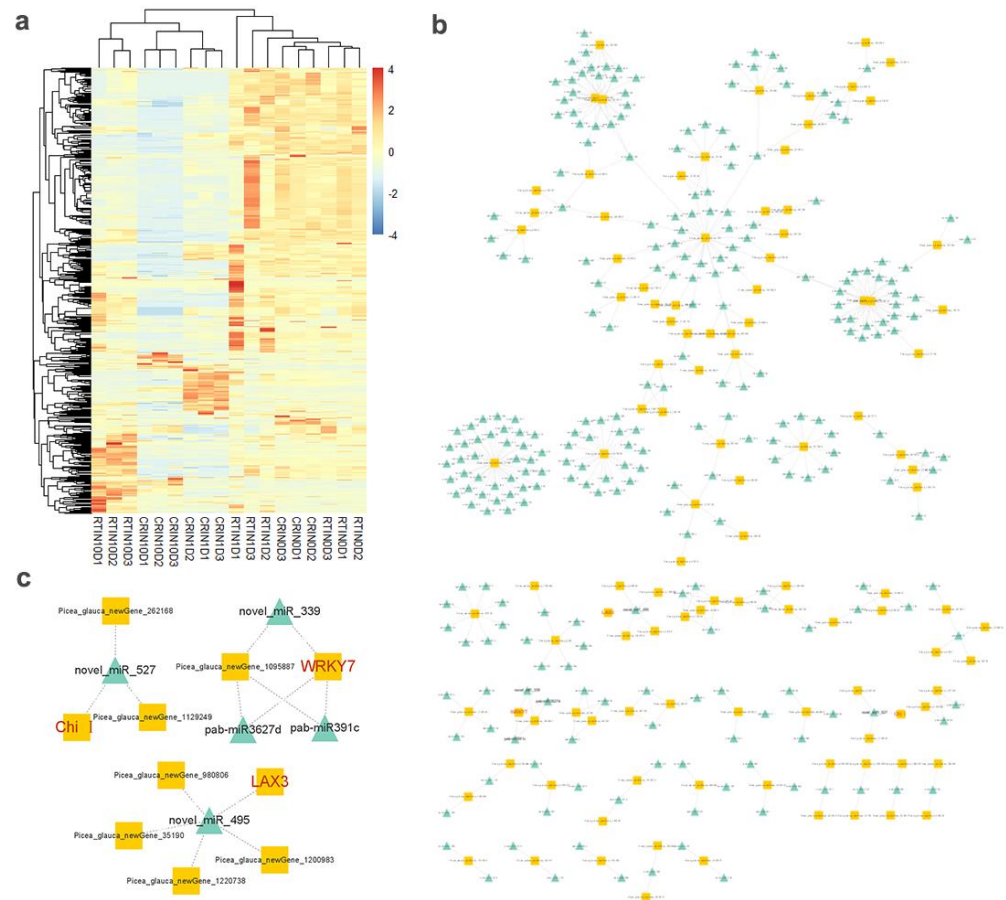


Figure 10. Analysis of DEMiRNAs (differentially expressed microRNAs) and targeted genes in blue module of WGCNA results: (a) hierarchical clustering of DEMiRNAs analysis; (b) network of miRNAs and targeted genes of blue module; blue triangle represents miRNAs, while yellow square represents targeted genes; (c) network of miRNAs and targeted hub genes; blue triangle represents miRNAs, and yellow square represents targeted genes.

3. Discussion

Somatic embryogenesis is an efficient means for mass propagation of coniferous species once the protocols are optimized as needed. Although CRSE and RTSE were both put on the same induction medium containing plant growth regulators, NET was easily induced from CRSE, instead of RTSE, which is mainly due to the liquid nitrogen treatment applied to the mature somatic embryos. It is well known that stress including wounding or exogenous hormones could trigger plant cell division and tissue regeneration [37]. Cells would be injured by the freezing treatment, insulating in the damage of plasma membrane, similar to dehydration or mechanical injury [5].

3.1. Application Value of Ultra-Low Temperature in Promoting ET Induction

This is the first report that cryo-treatment could enhance ET induction from mature somatic embryos in conifers. Compared with zygotic embryos, somatic embryos are visible and developing in *in vitro* conditions without a sampling window; in addition, mature somatic embryos, as sterile explant materials, could be inoculated into the induction medium with no need for sterilization, in contrast to zygotic ones. Furthermore, the genotype of mature somatic embryos is known and identical when the ET of known genotypes is used. On the contrary, zygotic embryos are obtained through pollination in nature, and the genotype of each zygotic embryo is different. Mature somatic embryos can also be preserved in liquid nitrogen for a long time during which elite genotypes can be screened by field test [3,4]. Then, mature somatic embryos of the selected genotype could be used for studies on the differences between genotypes and the propagation of conifers.

The previously reported results also showed that ET could be induced from mature zygotic embryos [5,6], and cold treatment could retain ET initiation capacity from zygotic embryos [38]; therefore, ultra-low temperature treatment might also be applied to mature zygotic embryos, which are cryo-tolerable, for a much better ET induction.

3.2. Effects of Cryo-Treatment and Exogenous Hormones on Gene Expression during the Induction from CRSE

The increased DNA methylation level of CRSE indicated that cryo-treatment caused stress to CRSE similarly to drought and salinity [39–41] at the early induction stage, which was important in initiating dedifferentiation. The highly expressed genes *OPT4*, *TIP1-1*, *Chi I*, *GST*, *WRKY7*, *MYBS3*, *LRR-RLK*, *PBL7*, and *WIN1* might be attributed to cryo-treatment during the CRSE induction process. *LRR-RLK* and *PBL7*, known as cytoplasmic membrane receptors, might function in signaling for subsequently activating plant defense mechanisms and controlling cell development, due to freezing treatment of CRSE [42,43]. Additionally, studies have shown that myo-Inositol phosphates are important for signaling processes in eukaryotes [44], suggesting that “inositol phosphate metabolism” also plays an important role in the signaling of NET induction. After receiving a signal from *RLK*, *MYBS3* and *WRKY7* genes regulate gene expression to promote resistance to cold stress [45–48]. In this study, a series of freeze-induced genes were regulated to enhance resistance. Firstly, specific messenger RNAs *WIN1* was largely induced after mechanical wounding due to cryo-treatment [49]; The accumulation of class I chitinases belonging to the *GH19* family was highly consistent with *WIN1* in plant defense against cold stress [50,51], which play important roles in the early developmental stage of somatic embryos [52]. *GST*, a soluble cytoplasmic enzyme, also played an important role in this resistant mechanism [53,54]. *TIP1-1* was responsible for water loss due to being frozen at liquid nitrogen [55]. *OPT4* proteins have transmembrane-spanning α -helical segments (TMSs) [56] and were also involved in stress response via transporting various substrates across the plasma membrane into the cell [57]. All these events might be connected closely with each other and play vital roles in the stress response of wounded somatic embryos.

Meanwhile, the exogenous hormone-induced genes *LAX3* were also highly expressed in the cryo-treated somatic embryos. In *Arabidopsis*, the auxin influx carrier gene *LAX3* induced by auxin promoted the development of lateral root primordia and apical hook [58–61],

while *GASA5* was localized to cell peripheries and could be upregulated by auxin and cytokinin, playing an important role in flowering time and seeds germination [62,63]. Although CRSE and RTSE were put on the same induction medium, the expression of genes *LAX3* and *GASA5* were notably lower in RTSE than CRSE, in particular, the expression of the *LAX3* gene, which decreased at day 10 in RTSE. Apart from the DNA methylation level profile, the reason why genes *LAX3* and *GASA5* expressed lower in RTSE might be that wounds resulting from ultra-low temperature treatment also caused epigenetic changes and cell reprogramming in CRSE.

3.3. CeRNA Network of lncRNAs, miRNAs, mRNAs during the Induction from CRSE

Non-coding RNAs, as epigenetic factors, could play important roles in regulating gene expression according to the present study. MicroRNAs could inhibit transcription or cleave genes to regulate gene expression level [64], while lncRNAs could protect gene expression by competing for endogenous RNA (ceRNA) for miRNAs, such as serving as miRNA sponges [25,65] or blocking the cleavage of pre-miRNAs [66].

In the current study, the expression level of lncRNA was highly intimated with gene expression, revealing that lncRNAs protected the expression of related genes in the process of NET induction of CRSE, such as *OPT4*, *TIP1-1*, *Chi I*, *GST*, *LAX3*, *WRKY7*, *LRR-RLK*, *PBL7*, and *WIN1* genes. Combined with miRNAs, the decreased expression level of novel miRNA 495 and the highly expressed *LAX3* gene illustrated that pre-novel_miR_495 might be bonded by lncRNAs MSTRG.33602.1 and MSTRG.1070680.1 to block the cleavage by DICER complex and protect the expression of related gene *LAX3*, increasing endogenous auxin levels and thus activating *GASA5* [67]. Similarly, lncRNA MSTRG.33602.1, MSTRG.505746.1, and MSTRG.1070680.1 might block the cleavage of pre-novel_miR_527 to protect the expression of *Chi I*, promoting the development of early somatic embryos [52]. However, the expression of novel_miR_339 was not negatively correlated with the targeted gene *WRKY7*, which was still highly expressed during the induction process. This phenomenon might be attributed to lncRNA MSTRG.33602.1, MSTRG.505746.1, and MSTRG.1070680.1, which, as miRNA sponges, could protect the expression of related gene *WRKY7*; then, the downstream genes of *WRKY7* such as *WIN1*, *OPT4*, *TIP1-1*, *Chi I*, and *GST* were regulated for stress response. Therefore, the successful induction of NET from CRSE was the result of the ceRNA network of lncRNAs, miRNAs, and mRNAs during the induction process (Figure 11).

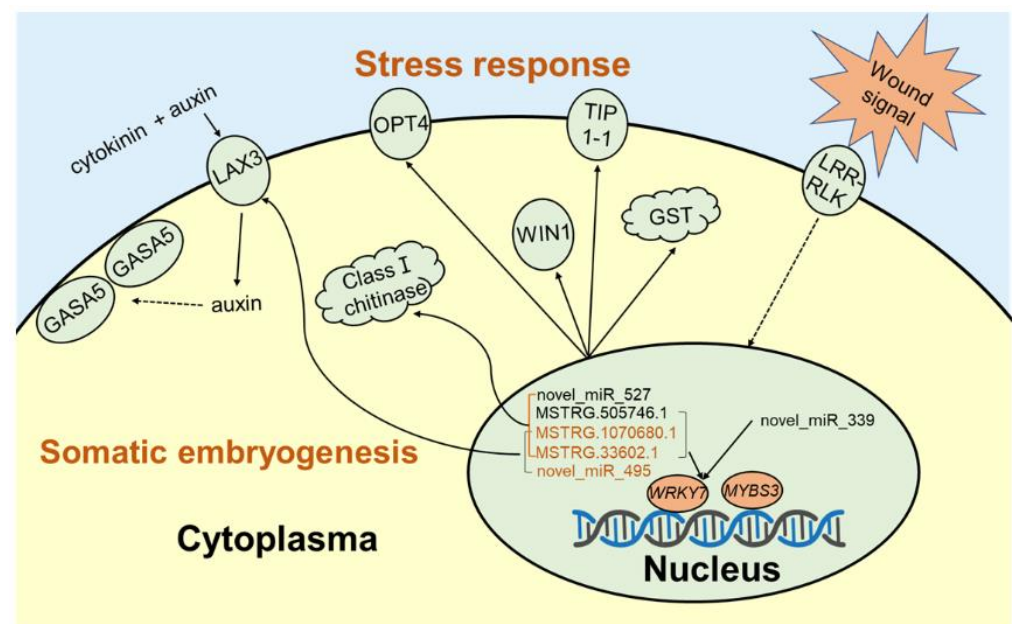


Figure 11. The proposed mechanism in the induction process of CRSE. The proposed mechanism in the induction process of CRSE, including oligopeptide transporter 4 (OPT4), aquaporin TIP1-1 (TIP1-1),

class I chitinase (Chi I), gibberellin-regulated protein 5 (GASA5), glutathione S-transferase (GST), auxin transporter-like protein 3 (LAX3), LRR receptor-like serine/threonine-protein kinase At1g07650 (LRR-RLK), serine/threonine-protein kinase PBL7 (PBL7) and x wound-induced protein WIN1 (PBL7), WRKY transcription factor 7 (WRKY7), Myb-related protein S3 (MYBS3), MSTRG.505746.1, MSTRG.1070680.1, MSTRG.33602.1, pab-miR391c, pab-miR3627d, novel_miR_339, novel_miR_47, and novel_miR_495.

4. Materials and Methods

4.1. Preparation of Plant Materials

The high-embryogenic cell line WSP17 of white spruce (*Picea glauca*) was selected and used for this study. The embryogenic tissues (ETs) were cultured on a half-strength modified Litvay (1/2 mLV) medium (1 mg/L 2,4-D, 0.5 mg/L 6-BA, 0.5 g/L hydrolyzed casein, 0.5 g/L glutamine, 10 g/L sucrose, 3 g/L gellan gum, pH 5.8) for maintenance and sub-cultured once two weeks at 23 ± 1 °C [68,69]. The ETs were transferred to liquid maintenance medium without gellan gum to suspend the embryogenic tissues and then moved to a pre-mature medium (1/2 mLV basal medium, 30 µM ABA, 0.4 g/L hydrolyzed casein, 0.5 g/L glutamine, 10 g/L sucrose, pH 5.8) for one week to promote early embryo development. To obtain the mature embryo, the embryogenic tissues were cultured on a mature medium (1/2 mLV basal medium, 45 µM ABA, 0.2 g/L hydrolyzed casein, 0.4 g/L glutamine, 30 g/L sucrose, 10 g/L maltose, 6 g/L gellan gum, pH 5.8) for 28 days. Somatic embryos were sampled and put into 1.5 mL sample tubes and then frozen in liquid nitrogen for 24 h, after which they were directly recovered for 5 min at 38 °C in a water bath. Lastly, the treated and untreated somatic embryos were put on an induction medium (1/2 mLV basal medium, 2 mg/L 2,4-D, 1 mg/L 6-BA, 0.5 g/L hydrolyzed casein, 0.5 g/L glutamine, 10 g/L sucrose, 3 g/L gellan gum, pH 5.8) and sampled at day 0, 1, 5, 10, and 20, respectively.

4.2. Microscopic Observation

The induction process was observed under dissecting microscopy (Leica Stereozoom S9i, Leica Co., Ltd., Germany, Wezlar). To further confirm the difference between cryo-treated somatic embryos (CRSEs) and normal somatic embryos cultured at room temperature at 23 ± 1 °C (RTSEs), during the induction for embryogenic tissue, samples were embedded in paraffin and dyed with safranin and fast green solution [70]. The DM6B Leica upright microscope (Leica Co., Ltd., Germany, Wezlar) was used for observing stained samples with a LAS X software image capture.

4.3. Detection of Induction Rate and Somatic Embryo Maturation Ability

The numbers of somatic embryos generated new embryogenic tissue (NET) and the total somatic embryos were counted for induction rate analysis, according to the following formula: induction rate = (the number of somatic embryos generated NET/the number of somatic embryos) \times 100%. Subsequently, the ET and NET obtained from CRSEs were transferred to a liquid maintenance medium, followed by a pre-matured medium, and finally, were cultured on the mature medium for four weeks. Then, the total number of somatic embryos was counted with 10 biological replicates, respectively. Lastly, we gathered the total number of somatic embryos per gram, which indicates the embryonic ability of ET.

4.4. Analysis of Global DNA Methylation

DNA was extracted from 200 mg samples of day 0, 1, 5, 10, 20 by using CTAB methods. Then, DNA was purified, hydrolyzed, and detected by a Waters E2695 HPLC instrument with a C18 column (Phenomenex 00G-4252-E0, 250 \times 4.6 mm, 5 µ), based on the protocol in Gao et al. [71], with minor modifications. DNA methylation level = (5 mC/(5 mC + C)) \times 100%. DNA methylation detection was conducted by three biological replications.

4.5. Whole-Transcriptome Sequencing

Samples obtained from day 0, 1, 10 in the induction process of RTSE and CRSE were used for RNA extraction at three biological replicates with RNA Extraction Kit (RN40, Aidlab Biotechnologies, Beijing, China), defined as RT0D, RT1D, RT10D, CR0D, CR1D, and CR10D. After sequencing on an Illumina Hiseq 2500 platform and eliminating the low-quality reads, HISAT2 [72] was used for mapping reads to the *Picea glauca* genome (GCA_000966675.2_WS77111_v2), and StringTie [73] was used for assembling mapped reads for mRNA and lncRNA analysis. The criteria of $|\text{fold change}| \geq 2$ & $\text{FDR} < 0.05$ was adopted for differential analysis of mRNA and lncRNA via DESeq2 [74]. For circRNA analysis, clean reads were also aligned to a pre-determined reference genome with BWA, in order to obtain their positions and specific sequence features. For siRNA analysis, Bowtie [75] was used for aligning sequence with Silva, GtRNAdb, Rfam, and RepBase databases, respectively; differential expression analysis was carried out by DESeq2 with $|\log_2(\text{FC})| \geq 0.58$ & $p\text{-value} \leq 0.05$.

4.6. Transcriptomic Co-Expression Network Analysis

The WGCNA R package (ver. 1.70-3) was utilized to construct the weighted gene co-expression network and divide related modules [76]. First, mRNAs with $|\text{(fold change)}| > 5$ were analyzed for correlation, and then, the power formula ($\text{adjacency} = (1 + \text{Pearson correlation})/2$) $^{|\beta|}$ was adopted for constructing the adjacency matrix. After determining soft threshold parameters β , the adjacency matrix was transformed into a topological overlap matrix, and the corresponding dissimilarity (1-TOM) was calculated. The minimum number of genes in the module was set to 30, and hierarchical clustering was carried out based on the TOM measurement method. Lastly, mRNAs with similar expression spectra were divided into the same module.

The lncRNA–mRNA co-expression network was constructed based on the correlation analysis between the differentially expressed lncRNAs and mRNAs. The expression of differentially expressed lncRNA and mRNAs were analyzed by Pearson's correlation coefficient with coefficient > 0.9 and $p\text{-value} < 0.01$. The targeted mRNAs of miRNAs were predicted by TargetFinder [59]. All the network maps were drawn by Cytoscape software (ver. 3.8.2).

4.7. Quantitative PCR Analysis

To validate the gene expression results of transcriptomes, qPCR was employed to determine the expression of genes on Applied Biosystems™ QuantStudio 6™ Real-Time PCR System (ABI, Carlsbad, CA, USA) by using Hieff UNICON Universal Blue SYBR Green Master Mix (Yeason Biotechnology Co., Ltd., Shanghai, China), according to the MIQE guidelines [77]. The PCR cycling conditions were 40 cycles of 95 °C for 30 s, 95 °C for 3 s, and 60 °C for 20 s. The expression profiles of lncRNAs were verified with Applied Biosystems™ QuantStudio 6™ Real-Time PCR System (ABI, Carlsbad, CA, USA) by using PerfectStart® Green qPCR SuperMix (+Dye II) (Transgene Biotechnology Co., Ltd., Beijing, China) according to manufacturer's protocol. The PCR cycling conditions were 40 cycles of 94 °C for 30 s, 94 °C for 5 s, and 60 °C for 34 s. The melting curves were analyzed during the reactions to ensure reaction specificity. The average expression level of three reference genes PaEF1, PsACTIN, PsUBQ gene [78–80] was used for the normalization of gene expression results (Table S1). PCR primers in Tables S2 and S3 were designed by primer blast (<https://www.ncbi.nlm.nih.gov/tools/primer-blast/>) with default parameters except for the product size (100–250 bp), and the primers were ordered from Tsingke BiotechCo., Ltd. (Beijing, China) qPCR analysis was performed in biological triplicate.

miRNAs were verified through poly (A) RT-qPCR [81] on Applied Biosystems™ QuantStudio 6™ Real-Time PCR System (ABI, Carlsbad, CA, USA) by using PerfectStart® Green qPCR SuperMix (+Dye II) (Transgene Biotechnology Co., Ltd., Beijing, China). In addition to using Pa5S, PatRNA-H1, PatRNA-R1 [82] as control samples (Table S1), PCR

primers in Table S4 were designed by the poly (A) RT-qPCR method. The PCR and calculation methods were similar to those of the lncRNAs.

4.8. Statistical Analysis

All experiments were replicated at least three times ($N \geq 3$), and all data were subjected to a two-way analysis of variance. The analysis of significant difference ($p < 0.05$) was carried out on SPSS 20 (IBM, Armonk, NY, USA) software via Duncan's multiple range test.

5. Conclusions

This is the first report that cryo-treatment of mature SE, as explants, enhanced ET induction in conifers. This method could be beneficial in genoplasm conservation and propagation of elite genotypes in conifers. The 5mC DNA methylation levels were noticeably altered differentially between the cryo-treated materials and the control during ET induction, which indicated that epigenetic factors might play important roles during the induction process. With whole-transcriptome technology and bioinformatic means, we found that ncRNAs, as epigenetic factors, critically affect the regulation of gene expressions such as lncRNAs and miRNAs. In this study, three lncRNAs (MSTRG.33602.1, MSTRG.505746.1, and MSTRG.1070680.1) and three miRNAs (novel_miR_339, novel_miR_495, and novel_miR_527) were selected by co-expression of lncRNA-mRNA and miRNA-mRNA in a blue module, and targeted at hub genes (*OPT4*, *TIP1-1*, *Chi I*, *GASA5*, *GST*, *LAX3*, *WRKY7*, *MYBS3*, *LRR-RLK*, *PBL7*, and *WIN1* genes). Results of this research revealed a probable regulation mechanism in the induction process using CRSE and provide insight into the initiation of early somatic embryogenesis in conifers. Additionally, the ultra-low temperature treatment might also be applied to mature zygotic embryos to increase the ET induction rate.

Supplementary Materials: The following supporting information can be downloaded at: <https://www.mdpi.com/article/10.3390/ijms23031111/s1>.

Author Contributions: L.K., Y.C., Y.G. and J.Z. (Jinfeng Zhang). designed the experiments; Y.C., Y.G., R.Z. and X.C. performed the experiments; Y.G. analyzed the data and prepared the manuscript draft; L.K., Y.G. and J.Z. (Jian Zhao) revised the manuscript. All authors have read and agreed to the published version of the manuscript.

Funding: This paper was funded by State Key Laboratory of Tree Genetics and Breeding (K2018202), National Key R&D Program of China (2017YDF0600404-1), the project fund (Somatic embryogenesis and high efficient propagation technology in trees) provided by Beijing Advanced Innovation Center for Tree Breeding by Molecular Design, the National Natural Science Foundation of China (31901289), Key R&D Program of Heibei Province, China (20326333D), Major Science and Technology Special Project of Xuchang, Henan province, China (20170112006).

Data Availability Statement: The datasets generated and/or analyzed during the current study are available from the corresponding author on reasonable request.

Acknowledgments: We would like to show our special thanks to Shen Zhou Lv Peng Agricultural Technology Co., Ltd. for all of the related supports.

Conflicts of Interest: The authors declare no conflict of interest.

References

1. Attree, S.M.; Fowke, L.C. Embryogeny of gymnosperms—Advances in synthetic seed technology of conifers. *Plant Cell Tissue Organ. Cult.* **1993**, *35*, 31–35. [[CrossRef](#)]
2. Park, Y.S.; Pond, S.E.; Bonga, J.M. Initiation of somatic embryogenesis in white spruce (*Picea glauca*): Genetic control, culture treatment effects, and implications for tree breeding. *Theor. Appl. Genet.* **1993**, *86*, 427–436. [[CrossRef](#)] [[PubMed](#)]
3. Park, Y.S.; Pond, S.E.; Bonga, J.M. Somatic embryogenesis in white spruce (*Picea glauca*): Genetic control in somatic embryos exposed to storage, maturation treatments, germination, and cryopreservation. *Theor. Appl. Genet.* **1994**, *89*, 742–750. [[CrossRef](#)]
4. Kong, L.; von Aderkas, P. A novel method of cryopreservation without a cryoprotectant for immature somatic embryos of conifer. *Plant. Cell Tissue Organ. Cult.* **2010**, *106*, 115–125. [[CrossRef](#)]
5. Tremblay, F.M. Somatic embryogenesis and plantlet regeneration from embryos isolated from stored seeds of *Picea glauca*. *Can. J. Bot.* **1990**, *68*, 236–242. [[CrossRef](#)]

6. Tao, J.; Chen, S.G.; Qin, C.Y.; Li, Q.M.; Cai, J.F.; Sun, C.; Wang, W.; Weng, Y. Somatic embryogenesis in mature zygotic embryos of *Picea pungens*. *Sci. Rep.* **2021**, *11*, 19072. [[CrossRef](#)] [[PubMed](#)]
7. Vondrakova, Z.; Cvikrova, M.; Eliasova, K.; Martincova, O.; Vagner, M. Cryotolerance in Norway spruce and its association with growth rates, anatomical features and polyamines of embryogenic cultures. *Tree Physiol.* **2010**, *30*, 1335–1348. [[CrossRef](#)] [[PubMed](#)]
8. Cui, Y.; Gao, Y.; Zhao, R.R.; Zhao, J.; Li, Y.X.; Qi, S.J.; Zhang, J.F.; Kong, L. Transcriptomic, metabolomic, and physiological analyses reveal that the culture temperatures modulate the cryotolerance and embryogenicity of developing somatic embryos in *Picea glauca*. *Front. Plant Sci.* **2021**, *12*, 694229. [[CrossRef](#)]
9. Klimaszewska, K.; Hargreaves, C.; Lelu-Walter, M.A.; Trontin, J.F. *Advances in Conifer Somatic Embryogenesis Since Year 2000*; Maria, A.G., Maurizio, L., Eds.; Springer Press: New York, NY, USA, 2016; Volume 1359, pp. 131–166.
10. Tretyakova, I.N.; Mineev, V.V. Reproductive potential of conifers, somatic embryogenesis and apomixis. *Russ. J. Dev. Biol.* **2021**, *52*, 75–86. [[CrossRef](#)]
11. Ikeda-Iwai, M.; Umehara, M.; Satoh, S.; Kamada, H. Stress-induced somatic embryogenesis in vegetative tissues of *Arabidopsis thaliana*. *Plant J.* **2003**, *34*, 107–114. [[CrossRef](#)]
12. Pais, M.S. Somatic embryogenesis induction in woody species: The future after OMICs data assessment. *Front. Plant Sci.* **2019**, *10*, 240. [[CrossRef](#)] [[PubMed](#)]
13. Ariel, F.; Romero-Barrios, N.; Jegu, T.; Benhamed, M.; Crespi, M. Battles and hijacks, noncoding transcription in plants. *Trends Plant Sci.* **2015**, *20*, 362–371. [[CrossRef](#)] [[PubMed](#)]
14. Cech, T.R.; Steitz, J.A. The noncoding RNA revolution—trashing old rules to forge new ones. *Cell* **2014**, *157*, 77–94. [[CrossRef](#)] [[PubMed](#)]
15. Li, C.; Wang, Z.K.; Zhang, J.J.; Zhao, X.Y.; Xu, P.; Liu, X.; Li, M.; Lv, C.; Song, X. Crosstalk of mRNA, miRNA, lncRNA, and circRNA and their regulatory pattern in Pulmonary fibrosis. *Mol. Ther. Nucleic Acids* **2019**, *18*, 204–218. [[CrossRef](#)]
16. D’Ario, M.; Griffiths-Jones, S.; Kim, M. Small RNAs: Big impact on plant development. *Trends Plant Sci.* **2017**, *22*, 1056–1068. [[CrossRef](#)] [[PubMed](#)]
17. Deng, P.C.; Liu, S.; Nie, X.J.; Song, W.S.; Wu, L. Conservation analysis of long non-coding RNAs in plants. *Sci. China Life Sci.* **2018**, *61*, 190–198. [[CrossRef](#)] [[PubMed](#)]
18. Salzman, J. Circular RNA expression: Its potential regulation and function. *Trends Genet.* **2016**, *32*, 309–316. [[CrossRef](#)]
19. Zhou, X.X.; Cui, J.; Meng, J.; Luan, Y.S. Interactions and links among the noncoding RNAs in plants under stresses. *Theor. Appl. Genet.* **2020**, *133*, 3235–3248. [[CrossRef](#)]
20. Chen, D.; He, B.; Zheng, P.; Wang, S.; Zhao, X.; Liu, J.; Yang, X.; Cheng, W. Identification of mRNA-, circRNA- and lncRNA-associated ceRNA networks and potential biomarkers for preeclampsia from umbilical vein endothelial cells. *Front. Mol. Biosci.* **2021**, *8*, 652250. [[CrossRef](#)]
21. Chen, Y.; Li, X.; Su, L.; Chen, X.; Zhang, S.; Xu, X.; Zhang, Z.; Chen, Y.; XuHan, X.; Lin, Y.; et al. Genome-wide identification and characterization of long non-coding RNAs involved in the early somatic embryogenesis in *Dimocarpus longan* Lour. *BMC Genom.* **2018**, *19*, 805. [[CrossRef](#)]
22. Song, J.H.; Cao, J.S. The progress of non-coding RNA in plants. *Biotechnol. Bull.* **2009**, *5*, 5–8.
23. Cao, P.; Fan, W.; Li, P.; Hu, Y. Genome-wide profiling of long noncoding RNAs involved in wheat spike development. *BMC Genom.* **2021**, *22*, 493. [[CrossRef](#)] [[PubMed](#)]
24. Pan, W.J.; Tao, J.J.; Cheng, T.; Bian, X.H.; Wei, W.; Zhang, W.K.; Ma, B.; Chen, S.Y.; Zhang, J.S. Soybean miR172a improves salt tolerance and can function as a long-distance signal. *Mol. Plant.* **2016**, *9*, 1337–1340. [[CrossRef](#)]
25. Zhao, Z.; Sun, W.; Guo, Z.Y.; Zhang, J.C.; Yu, H.G.; Liu, B. Mechanisms of lncRNA/microRNA interactions in angiogenesis. *Life Sci.* **2020**, *254*, 116900. [[CrossRef](#)] [[PubMed](#)]
26. Gao, Z.; Li, J.; Luo, M.; Li, H.; Chen, Q.; Wang, L.; Song, S.; Zhao, L.; Xu, W.; Zhang, C.; et al. Characterization and cloning of grape circular RNAs identified the cold resistance-related *Vv-circATS1*. *Plant Physiol.* **2019**, *180*, 966–985. [[CrossRef](#)] [[PubMed](#)]
27. Wu, X.M.; Liu, M.Y.; Ge, X.X.; Xu, Q.A.; Guo, W.W. Stage and tissue-specific modulation of ten conserved miRNAs and their targets during somatic embryogenesis of *Valencia* sweet orange. *Planta* **2011**, *233*, 495–505. [[CrossRef](#)] [[PubMed](#)]
28. Su, Y.H.; Liu, Y.B.; Zhou, C.; Li, X.M.; Zhang, X.S. The microRNA167 controls somatic embryogenesis in *Arabidopsis* through regulating its target genes *ARF6* and *ARF8*. *Plant Cell Tissue Organ. Cult.* **2016**, *124*, 405–417. [[CrossRef](#)]
29. Lujan-Soto, E.; Juarez-Gonzalez, V.T.; Reyes, J.L.; Dinkova, T.D. MicroRNA Zma-miR528 versatile regulation on target mRNAs during maize somatic embryogenesis. *Int. J. Mol. Sci.* **2021**, *22*, 5310. [[CrossRef](#)]
30. Zhang, J.H.; Wu, T.; Li, L.; Han, S.Y.; Li, X.M.; Zhang, S.; Qi, L. Dynamic expression of small RNA populations in larch (*Larix leptolepis*). *Planta* **2013**, *237*, 89–101. [[CrossRef](#)]
31. Yakovlev, I.A.; Fossdal, C.G. In silico analysis of small RNAs suggest roles for novel and conserved miRNAs in the formation of epigenetic memory in somatic embryos of Norway spruce. *Front. Physiol.* **2017**, *8*, 674. [[CrossRef](#)] [[PubMed](#)]
32. Li, Q.F.; Deng, C.; Zhu, T.Q.; Ling, J.J.; Zhang, H.G.; Kong, L.; Zhang, S.; Wang, J.; Chen, X. Dynamics of physiological and miRNA changes after long-term proliferation in somatic embryogenesis of *Picea balsamifera*. *Trees* **2019**, *33*, 469–480. [[CrossRef](#)]
33. Hu, X.G.; Zhou, S.S.; Yang, Y.; Liu, H.; Anil, S.; Wang, Q.; Zhao, W.; Gao, Q.; El-Kassaby, Y.A.; Wang, T.; et al. Transcriptome-wide identification and profiling of miRNAs in a stress-tolerant conifer *Sabina chinensis*. *J. Biosci.* **2020**, *45*, 41. [[CrossRef](#)]

34. Perdiguero, P.; Rodrigues, A.S.; Chaves, I.; Costa, B.; Alves, A.; de Maria, N.; Vélez, M.D.; Díaz-Sala, C.; Cervera, M.T.; Miguel, C.M. Comprehensive analysis of the isomiRome in the vegetative organs of the conifer *Pinus pinaster* under contrasting water availability. *Plant Cell Environ.* **2021**, *44*, 706–728. [[CrossRef](#)] [[PubMed](#)]
35. Varhanikova, M.; Uvackova, L.; Skultety, L.; Pretova, A.; Obert, B.; Hajduch, M. Comparative quantitative proteomic analysis of embryogenic and non-embryogenic calli in maize suggests the role of oxylipins in plant totipotency. *J. Proteom.* **2014**, *104*, 57–65. [[CrossRef](#)] [[PubMed](#)]
36. Wen, L.; Li, W.; Parris, S.; West, M.; Lawson, J.; Smathers, M.; Li, Z.; Jones, D.; Jin, S.; Saski, C.A. Transcriptomic profiles of non-embryogenic and embryogenic callus cells in a highly regenerative upland cotton line (*Gossypium hirsutum* L.). *BMC Dev. Biol.* **2020**, *20*, 25. [[CrossRef](#)] [[PubMed](#)]
37. Lee, K.; Park, O.S.; Lee, H.G.; Seo, P.J. The ASHR3 SET-domain protein is a pivotal upstream coordinator for wound-induced callus formation in *Arabidopsis*. *J. Plant Biol.* **2020**, *63*, 361–368. [[CrossRef](#)]
38. Hely, H.; Anne, J.; Jana, K.; Anneli, K.; Karoliina, N.; Aronen, T. Somatic embryogenesis of Scots pine: Cold treatment and characteristics of explants affecting induction. *J. Exp. Bot.* **1999**, *50*, 1769–1778.
39. Lan, Z.; Xu, Y.H.; Wang, J.B. DNA-methylation changes induced by salt stress in wheat *Triticum aestivum*. *Afr. J. Biotechnol.* **2009**, *8*, 6201–6207. [[CrossRef](#)]
40. Joel, G.A.J. Epigenetic responses to drought stress in rice (*Oryza sativa* L.). *Physiol. Mol. Biol. Plants* **2013**, *19*, 379–387.
41. Falahi, A.; Zarei, L.; Cheghamirza, K. Most drought-induced DNA methylation changes switched to pre-stress state after re-irrigation in barley (*Hordeum vulgare* L.) cultivars. *Cereal Res. Commun.* **2021**, *10*. [[CrossRef](#)]
42. Lease, K.A.; Lau, N.Y.; Schuster, R.A.; Torii, K.U.; Walker, J.C. Receptor serine/threonine protein kinases in signalling: Analysis of the erecta receptor-like kinase of *Arabidopsis thaliana*. *New Phytol.* **2001**, *151*, 133–143. [[CrossRef](#)]
43. Afzal, A.J.; Wood, A.J.; Lightfoot, D.A. Plant receptor-like serine threonine kinases: Roles in signaling and plant defense. *Mol. Plant Microb. Interact.* **2008**, *21*, 507–517. [[CrossRef](#)]
44. Khodakovskaya, M.; Sword, C.; Wu, Q.; Perera, I.Y.; Boss, W.F.; Brown, C.S.; Winter Sederoff, H. Increasing inositol (1,4,5)-trisphosphate metabolism affects drought tolerance, carbohydrate metabolism and phosphate-sensitive biomass increases in tomato. *Plant Biotechnol. J.* **2010**, *8*, 170–183. [[CrossRef](#)] [[PubMed](#)]
45. Su, C.F.; Wang, Y.C.; Hsieh, T.H.; Lu, C.A.; Tseng, T.H.; Yu, S.M. A novel MYBS3-dependent pathway confers cold tolerance in rice. *Plant Physiol.* **2010**, *153*, 145–158. [[CrossRef](#)] [[PubMed](#)]
46. Zhang, T.; Zhao, X.Q.; Wang, W.S.; Pan, Y.J.; Huang, L.Y.; Liu, X.; Zong, Y.; Zhu, L.; Yang, D.; Fu, B. Comparative transcriptome profiling of chilling stress responsiveness in two contrasting rice genotypes. *PLoS ONE* **2012**, *7*, e43274. [[CrossRef](#)]
47. He, X.; Li, J.J.; Chen, Y.; Yang, J.; Chen, X.Y. Genome-wide analysis of the WRKY gene family and its response to abiotic stress in buckwheat (*Fagopyrum Tataricum*). *Open Life Sci.* **2019**, *14*, 80–96. [[CrossRef](#)]
48. Baillo, E.H.; Hanif, M.S.; Guo, Y.; Zhang, Z.; Xu, P.; Algam, S.A. Genome-wide Identification of WRKY transcription factor family members in sorghum (*Sorghum bicolor* (L.) moench). *PLoS ONE* **2020**, *15*, e0236651.
49. Stanford, A.; Bevan, M.; Northcote, D. Differential expression within a family of novel wound-induced genes in potato. *Mol. Gen. Genet.* **1989**, *215*, 200–208. [[CrossRef](#)] [[PubMed](#)]
50. Xu, Z.N.; Pu, L.M.; Qu, Y.; Yang, Y.; Bai, Z.W.; Guan, R.P.; Zhang, Q.; Cui, X.M.; Liu, D.Q. Cloning and expression analysis of a chitinase gene PnCHI1 from *Panax notoginseng*. *China J. Chin. Mater. Med.* **2016**, *41*, 20.
51. Rajninc, M.; Jopcik, M.; Danchenko, M.; Libantova, J. Biochemical and antifungal characteristics of recombinant class I chitinase from *Drosera rotundifolia*. *Int. J. Biol. Macromol.* **2020**, *161*, 854–863. [[CrossRef](#)] [[PubMed](#)]
52. Kragh, K.M.; Hendriks, T.; de Jong, A.J.; Lo Schiavo, F.; Bucherna, N.; Højrup, P.; Mikkelsen, J.D.; de Vries, S.C. Characterization of chitinases able to rescue somatic embryos of the temperature-sensitive carrot variant ts 11. *Plant Mol. Biol.* **1996**, *31*, 631–645. [[CrossRef](#)] [[PubMed](#)]
53. Mohsenzadeh, S.; Esmaeili, M.; Moosavi, F.; Shahrtash, M.; Saffari, B.; Mohabatkar, H. Plant glutathione S-transferase classification, structure and evolution. *Afr. J. Biotechnol.* **2011**, *10*, 8160–8165.
54. Wang, J.R.; Zhang, Z.; Wu, J.H.; Han, X.Y.; Wang-Pruski, G.F.; Zhang, Z. Genome-wide identification, characterization, and expression analysis related to autotoxicity of the GST gene family in *Cucumis melo* L. *Plant Physiol. Biochem.* **2020**, *155*, 59–69. [[CrossRef](#)]
55. Medina, S.; Vicente, R.; Nieto-Taladriz, M.T.; Aparicio, N.; Chairi, F.; Vergara-Diaz, O.; Araus, J.L. The plant-transpiration response to vapor pressure deficit (VPD) in durum wheat is associated with differential yield performance and specific expression of genes involved in primary metabolism and water transport. *Front. Plant Sci.* **2018**, *9*, 1994. [[CrossRef](#)] [[PubMed](#)]
56. Gomolplitinant, K.M.; Saier, M.H.J. Evolution of the oligopeptide transporter family. *J. Membrane Biol.* **2011**, *240*, 89–110. [[CrossRef](#)] [[PubMed](#)]
57. Xiang, Q.J.; Shen, K.Y.; Yu, X.M.; Zhao, K.; Gu, Y.F.; Zhang, X.; Chen, X.; Chen, Q. Analysis of the oligopeptide transporter gene family in *Ganoderma lucidum*: Structure, phylogeny, and expression patterns. *Genome* **2017**, *60*, 293–302. [[CrossRef](#)]
58. Swarup, K.; Benkova, E.; Swarup, R.; Casimiro, I.; Péret, B.; Yang, Y.; Parry, G.; Nielsen, E.; De Smet, I.; Vanneste, S.; et al. The auxin influx carrier LAX3 promotes lateral root emergence. *Nat. Cell Biol.* **2008**, *10*, 946–954. [[CrossRef](#)]
59. Shen, C.J.; Bai, Y.H.; Wang, S.K.; Zhang, S.N.; Wu, Y.R.; Chen, M.; Jiang, D.; Qi, Y. Expression profile of PIN, AUX/LAX and PGP auxin transporter gene families in *Sorghum bicolor* under phytohormone and abiotic stress. *FEBS J.* **2010**, *277*, 2954–2969. [[CrossRef](#)]

60. Vandenbussche, F.; Petrasek, J.; Zadnikova, P.; Hoyerová, K.; Pesek, B.; Raz, V.; Swarup, R.; Bennett, M.; Zažímalová, E.; Benková, E.; et al. The auxin influx carriers AUX1 and LAX3 are involved in auxin-ethylene interactions during apical hook development in *Arabidopsis thaliana* seedlings. *Development* **2010**, *137*, 597–606. [[CrossRef](#)]
61. da Costa, C.T.; Offringa, R.; Fett-Neto, A.G. The role of auxin transporters and receptors in adventitious rooting of *Arabidopsis thaliana* pre-etiolated flooded seedlings. *Plant Sci.* **2020**, *290*, 110294. [[CrossRef](#)]
62. Qu, J.; Kang, S.G.; Hah, C.; Jang, J.C. Molecular and cellular characterization of GA-stimulated transcripts *GASA4* and *GASA6* in *Arabidopsis thaliana*. *Plant Sci.* **2016**, *246*, 1–10. [[CrossRef](#)]
63. Zhong, C.; Patra, B.; Tang, Y.; Li, X.; Yuan, L.; Wang, X. A transcriptional hub integrating gibberellin-brassinosteroid signals to promote seed germination in *Arabidopsis*. *J. Exp. Bot.* **2021**, *72*, 4708–4720. [[CrossRef](#)]
64. Allen, E.; Xie, Z.; Gustafson, A.M.; Carrington, J.C. microRNA-directed phasing during trans-acting siRNA biogenesis in plants. *Cell* **2005**, *121*, 207–221. [[CrossRef](#)]
65. Lu, Q.; Xu, Q.; Guo, F.; Lv, Y.; Song, C.; Feng, M.; Yu, J.; Zhang, D.; Cang, J. Identification and characterization of long non-coding RNAs as competing endogenous RNAs in the cold stress response of *Triticum aestivum*. *Plant Biol.* **2020**, *22*, 635–645. [[CrossRef](#)] [[PubMed](#)]
66. Tian, T.; Lv, X.B.; Pan, G.K.; Lu, Y.J.; Chen, W.X.; He, W.; Lei, X.; Zhang, H.; Liu, M. Long noncoding RNA MPRL promotes mitochondrial fission and cisplatin chemosensitivity via disruption of pre-miRNA processing. *Clin. Cancer Res.* **2019**, *25*, 3673–3688. [[CrossRef](#)] [[PubMed](#)]
67. Hoyerová, K.; Perry, L.; Hand, P.; Lanková, M.; Kocábek, T.; May, S.; Kottová, J.; Paces, J.; Napier, R.; Zazimalova, E. Functional characterization of PaLAX1, a putative auxin permease, in heterologous plant systems. *Plant Physiol.* **2008**, *146*, 1128–1141. [[CrossRef](#)] [[PubMed](#)]
68. Litvay, J.D.; Verma, D.C.; Johnson, M.A. Influence of a loblolly pine (*Pinus taeda* L.) Culture medium and its components on growth and somatic embryogenesis of the wild carrot (*Daucus carota* L.). *Plant Cell Rep.* **1985**, *4*, 325–328. [[CrossRef](#)]
69. Kong, L.; von Aderkas, P. Genotype effects on ABA consumption and somatic embryo maturation in interior spruce (*Picea glauca* × *engelmanni*). *J. Exp. Bot.* **2007**, *58*, 1525–1531. [[CrossRef](#)]
70. Chen, H.M.; Rui, J.S.; Tang, J.H. Safranin O and fast green FCF. *J. Biol.* **1989**, *2*, 33–34.
71. Gao, Y.; Hao, J.L.; Wang, Z.; Song, K.J.; Ye, J.H.; Zheng, X.Q.; Liang, Y.R.; Lu, J.L. DNA methylation levels in different tissues in tea plant via an optimized HPLC method. *Horticult. Environ. Biotech.* **2019**, *60*, 967–974. [[CrossRef](#)]
72. Li, J.; Ma, W.; Zeng, P.; Wang, J.; Geng, B.; Yang, J.; Cui, Q. LncTar: A tool for predicting the RNA targets of long noncoding RNAs. *Brief. Bioinform.* **2014**, *16*, 806–812. [[CrossRef](#)]
73. Kim, D.; Langmead, B.; Salzberg, S.L. HISAT: A fast spliced aligner with low memory requirements. *Nat. Methods* **2015**, *12*, 357–360. [[CrossRef](#)]
74. Love, M.I.; Huber, W.; Anders, S. Moderated estimation of fold change and dispersion for RNA-seq data with DESeq2. *Genome Biol.* **2014**, *15*, 550. [[CrossRef](#)] [[PubMed](#)]
75. Langmead, B.; Trapnell, C.; Pop, M.; Salzberg, S.L. Ultrafast and memory-efficient alignment of short DNA sequences to the human genome. *Genome Biol.* **2009**, *10*, R25. [[CrossRef](#)] [[PubMed](#)]
76. Langfelder, P.; Horvath, S. WGCNA: An R package for weighted correlation network analysis. *BMC Bioinform.* **2008**, *9*, 559. [[CrossRef](#)]
77. Bustin, S.A.; Benes, V.; Garson, J.A.; Hellemans, J.; Huggett, J.; Kubista, M.; Mueller, R.; Nolan, T.; Pfaffl, M.W.; Shipley, G.L.; et al. The MIQE guidelines: Minimum information for publication of quantitative real-time PCR experiments. *Clin. Chem.* **2009**, *55*, 611–622. [[CrossRef](#)] [[PubMed](#)]
78. Vuosku, J.; Sarjala, T.; Jokela, A.; Sutela, S.; Saaskilahti, M.; Suorsa, M.; Läärä, E.; Häggman, H. One tissue, two fates: Different roles of megagametophyte cells during Scots pine embryogenesis. *J. Exp. Bot.* **2009**, *60*, 1375–1386. [[CrossRef](#)]
79. Vestman, D.; Larsson, E.; Uddenberg, D.; Cairney, J.; Clapham, D.; Sundberg, E.; von Arnold, S. Important processes during differentiation and early development of somatic embryos of Norway spruce as revealed by changes in global gene expression. *Tree Genet. Genomes* **2011**, *7*, 347–362. [[CrossRef](#)]
80. Alakarppa, E.; Salo, H.M.; Valledor, L.; Canal, M.J.; Haggman, H.; Vuosku, J. Natural variation of DNA methylation and gene expression may determine local adaptations of Scots pine populations. *J. Exp. Bot.* **2018**, *69*, 5293–5305. [[CrossRef](#)]
81. Shi, R.; Yang, C.; Sederoff, R.; Chiang, V. Validation of artificial microRNA expression by poly(A) tailing-based RT-PCR. *Nat. Protoc.* **2012**. [[CrossRef](#)]
82. Yakovlev, I.A.; Fossdal, C.G.; Johnsen, Ø. MicroRNAs, the epigenetic memory and climatic adaptation in Norway spruce. *New Phytol.* **2010**, *187*, 1154–1169. [[CrossRef](#)] [[PubMed](#)]